Expanded View Figures

Figure EV1. Expression analysis and growth characteristics of mutants used in this study.
All strains are listed in Appendix Table S1.

A Mutations in the Dsl1p lasso domain and the deletion of the lasso domain do not affect the stability of the protein. Since Dsl1p antibodies preferentially recognize the Dsl1 protein carrying an intact lasso domain, we analyzed myc-tagged proteins. The sequences encoding two myc-tags were introduced 3′ of the *DSL1* alleles as described in Materials and Methods. Extracts of two parallel samples were analyzed using the 9B11 antibody (Cell Signaling Technologies, Danvers, MA). δ-COP was used as a loading control. As an additional loading control, a Ponceau S-stained protein band at about 120 kDa is shown.

B, C Immunoblot analysis of strains expressing either VN or VC tags alone. For the upper panels, COPI-specific antibodies were used and untagged COPI subunits were employed as a loading control. For the blots shown in the second row, GFP-specific antibodies were used. As an additional loading control, a Ponceau S-stained protein band at about 120 kDa is shown. The results indicate that expression of α-COP and β′-COP is not affected by the tags, while the tagged versions of genes encoding δ-COP and ε-COP seem to be less well expressed. We do not know why the expression varies so much since all tagged genes except *RER1* are under the control of their own promoter, and all 3′-tagged genes are followed by the *ADH1* 3′-UTR. Our results with *VC-RER1* indicate that the codon usage of the tag may be important at least when the tag is at the 5′ end (Lipatova *et al*, 2015). We obtained very similar results when we used a chromosomally inserted *VC-RER1* version under the control of the strong RPL7B promoter or a single-copy vector-encoded version under the endogenous promoter where the codon usage of the VC tag was adapted to yeast.

D, E The formation of BiFC complexes has no effect on the expression of the modified proteins. Blots show extracts from individually tagged strains as well as strains expressing BiFC pairs. The BiFC combinations Dsl1p^{VN}•ε-COP^{VC} and β′-COP^{VN}•Dsl3p^{VC} shown here were those which we used most often in this work for microscopy. They represent BiFC pairs with either a poorly or a well-expressed BiFC-tagged COPI subunit. As a loading control, a Ponceau S-stained protein band at about 120 kDa is shown.

F *RER1* carrying the VC tag at its 5′ end was expressed under the control of the strong RPL7B promoter. The full-length fusion protein is present in amounts comparable to the wild-type protein. A smaller protein fragment is very likely the product of cleavage by vacuolar proteases (Sato *et al*, 2001). The antibody used was raised against the C-terminal 27 residues of Rer1p (Boehm *et al*, 1997). As a loading control, a Ponceau S-stained protein band at about 120 kDa is shown.

G Dsl1p and Dsl3p levels do not change significantly when they carry BiFC tags or when expressed as BiFC pairs. Antibodies raised against the full-length proteins were used for this analysis. Apart from δ-COP, the area around a 70 kDa band of the Ponceau S-stained blots is shown as a loading control.

H Growth assays with strains expressing different BiFC combinations. The cell density of exponentially growing cells was adjusted to 1 OD_{600}. These suspensions as well as three serial dilutions were spotted on agar plates. Images were taken after 48 h incubation at the indicated temperature. Rer1p marked with one asterisk indicates that the VC-tagged *RER1* gene was expressed under the control of the RPL7B promoter from the *RER1* locus. The plasmid-encoded version with codon-adapted VC tag under the control of the endogenous promoter is marked by two asterisks. The growth test shown was performed on selective minimal medium to prevent the loss of plasmids.

I The β′-COP^{VN}•Dsl3p^{VC} BiFC pair does not interfere with the binding of the Dsl complex to the SNARE protein Sec20p. Tandem affinity-purified Sec20p^{TAP} containing complexes from radiolabeled BiFC and non-BiFC cells were isolated as described previously (Kraynack *et al*, 2005). The BiFC pair used was the β′-COP^{VN}•Dsl3p^{VC} combination. Note that no matter whether the TAP-tag was at the C-terminus of Sec20p (first lane) or Dsl1p (third lane), comparable amounts of COPI subunits co-purified with the tagged protein. As a control, *SEC20*-TAP cells were analyzed which carried no BiFC combination (second lane). Very little Sec20p^{TAP} was visible due to the low amount of Cys and Met residues. We used immunoblot analysis to confirm that the tagged protein is produced. Tandem affinity-purified complexes were analyzed by SDS–PAGE. Gels were dried and analyzed using a phosphorimager (FLA7000, Fujifilm).

J Emp47p levels are reduced to about 60% of the wild-type level in β′-COP^{VN} expressing cells. We observed a reduction in the Emp47p level in extracts from cells with different BiFC combinations (H.D. Schmitt, unpublished results). This was not observed when strains produced β′-COP fused to full-length GFP. Thus, it was not simply the size of the tag that caused the effect. Using extracts from six wild-type, six β′-COP^{VN}, and six β′-COP^{VN}•Dsl3^{VC} strains from older as well as fresh crosses, our immunoblot analysis clearly showed that the reduction in the Emp47p level was not due to the BiFC formation. It can already be observed in β′-COP^{VN}-producing cells. The blots were analyzed using a Lumi-Imager camera system and quantified using the Lumi-Imager software (Roche). Hexokinase was used as a loading control. The stability of the Rer1 protein was not affected.

K The presence of untagged proteins in addition to the VC-tagged Dsl proteins reduces the BiFC signal, while it does not change the polarized appearance of BiFC spots. For the micrographs shown, diploid strains were imaged that express VN-tagged β′-COP from both *SEC27* loci. At the *DSL3* loci, they express a wild-type and a VC-tagged version (upper panel) or two *DSL3*^{VC} alleles (lower panel). The same result was obtained with strains that are heterozygous or homozygous for the equivalent *DSL1* versions. Moreover, a β′-COP^{VN}/β′-COP^{VN}, *DSL1*^{VN}/*DSL1*, *DSL3*^{VN}/*DSL3* strain could not be distinguished from a homozygous β′-COP^{VN}/β′-COP^{VN} *DSL3*^{VN}/*DSL3*^{NV} strain (H.D. Schmitt, unpublished results). Thus, the BiFC spot formation is not due to a depletion of Dsl proteins. Scale bar, 5 μm.

L PLA detection of COPI/Dsl and COPI/ER-SNARE interactions. Superimposed representative images of fixed yeast cells carrying Dsl3p^{GFP}, Sec20p^{GFP}, or no tag (wild type). Cells were fixed with PFA and immunodecorated with primary antibodies against endogenous COPI, as well as GFP. Subsequently, the PLA reaction was carried out according to the manufacturer's instructions, using Duolink® *In Situ* red PLA reagents. Proximity of COPI to Dsl3p^{GFP} or Sec20p^{GFP} produced to a fluorescent spot *in situ*. Gray channel: DIC; blue: DAPI; red: PLA signal. Scale bar, 10 μm.

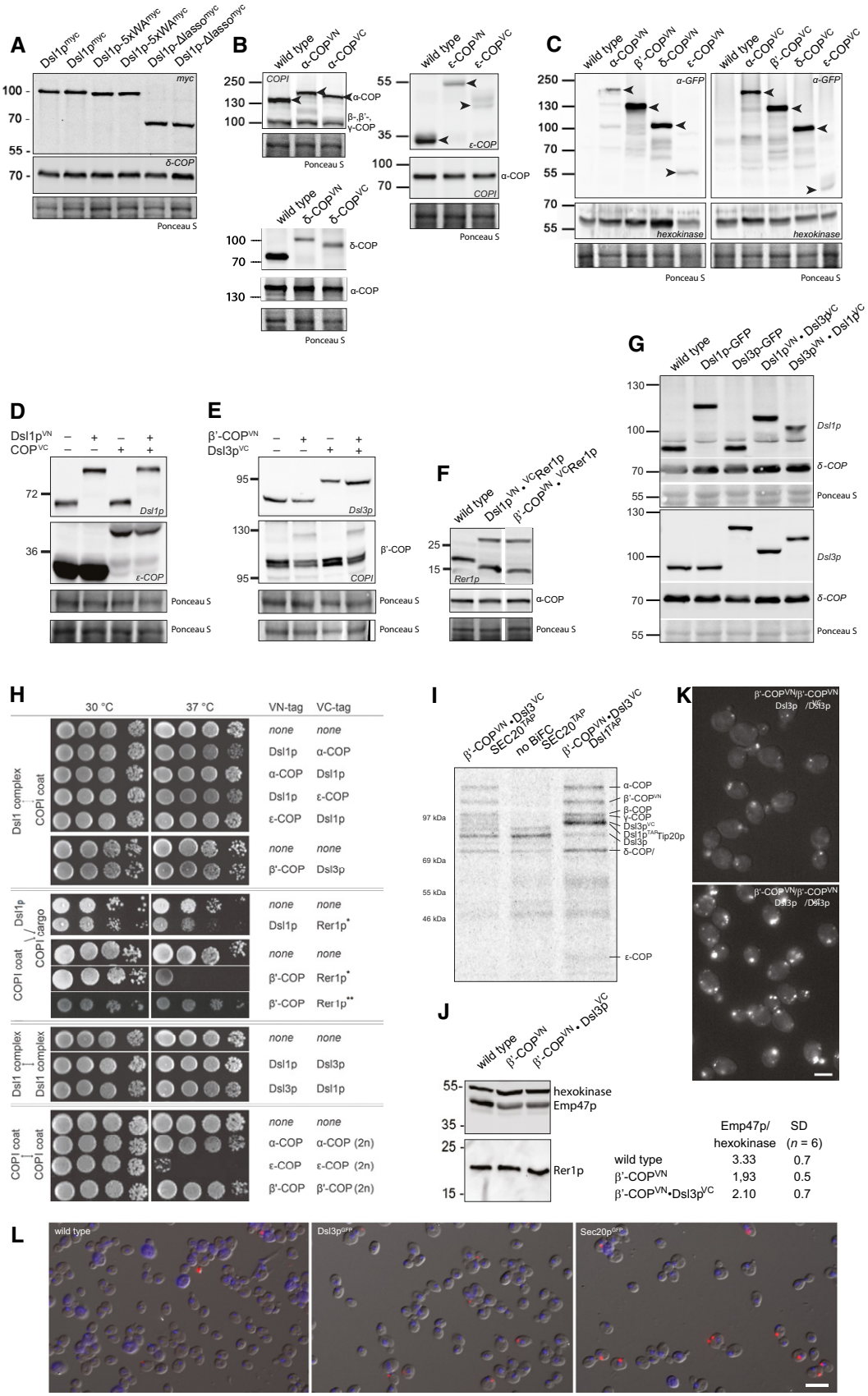

Figure EV1.

Figure EV2. COPI•Dsl BiFC interactions can suppress lethal combinations of *dsl1* mutations and unpaired VN tags.

The heat maps in this figure represent a summary of the growth assays shown in Appendix Fig S1 (representative data are shown in Fig 1F). Growth in successive dilution spots was scored (green: full growth compared to control strain, red: complete inability to grow). The cells carried either the wild-type *DSL1* gene or one of two different *dsl1* mutations. Lettering of the datasets is in accordance with Appendix Fig S1. The results indicate that the *dsl1* mutations are in fact lethal in combination with all VN-tagged COPI subunits. This is suppressed by the presence of the VC tag at Dsl subunits and, very importantly, only the Dsl proteins. See the Appendix for further discussion of these results.

A Plasmid-encoded wild-type and mutant versions of *DSL1* support growth of *DSL1* shutoff cells that carry no other modification.

B The presence of unpaired VN tags at the C-terminus of α-, β'-, δ-, and ε-COP was lethal when combined with the *dsl1-5xWA* mutation. Cells producing α-COP^{VN} were temperature-sensitive no matter what *DSL1* version was present in the cells. δ-COP^{VN}-producing cells were also temperature-sensitive, but a surplus of Dsl1p suppressed the temperature sensitivity.

C Compared to the VN tag, the VC fragment at the C-terminus of COPI subunits had a less dramatic effect on growth when combined with the *dsl1-5xWA* mutation. Cells producing δ-COP^{VC} were an exception. The δ-COP^{VC} cells were temperature-sensitive no matter what *DSL1* version was expressed. It has been observed previously that δ-COP^{GFP} cells are also temperature-sensitive (Zink *et al*, 2009; see also F and G).

D No synthetic lethality was observed when the *dsl1-5xWA* mutation was expressed in cells with VN or VC tags at the C-terminus of Dsl proteins or COPII subunits Sec24p and Sec16p. However, cells expressing a VN or VC-tagged dsl1-5xWA protein grew slower than the corresponding wild-type version even at room temperature.

E The lethal COPI/*dsl1-5xWA* combinations shown in (B) were viable when *DSL3*^{VC} was expressed as well, suggesting that the BiFC interaction can reconstitute the normal function of the coat/tether interaction. Note that the β'-COP^{VN}•Dsl3p^{VC} combination, which includes the most efficiently expressed BiFC-tagged COPI subunit, grew well even at 37°C (see also Fig 1F), while the combination that includes the β'-COP$^{VN\ I152L}$ version could not grow at 37°C. As discussed below, this observation indicates that for suppression to occur, it is optimal if the BiFC formation is very efficient.

F As shown in (C), cells with VC-tagged δ-COP stopped growing when the *dsl1-5xWA* mutant allele was the only *DSL1* version expressed in the cells. The growth of these cells was improved by the VN tag fused to Dsl1p (compare the last rows of C and F). This effect was limited to 30°C since the cells were temperature-sensitive.

G Dsl1p carrying the VC tag rescued two of the four COPI^{VN}/*dsl1-5xWA* combinations (ε-COP^{VN} and β'-COP^{VN}). In contrast to *DSL3*^{VC}, *DSL1*^{VN} could not suppress the equivalent combinations with α-COP^{VN} and δ-COP^{VN}. For these tests, a plasmid-encoded VC-tagged version of *dsl1-5xWA* was used. The failure of this plasmid to support growth of α-COP^{VN} and δ-COP^{VN} producing cells may indicate that *DSL1*^{VN} is less efficient as suppressor than *DSL3*^{VN}. However, one must keep in mind that the BiFC tags fused to the dsl1-5xWA protein alone caused a growth defect (D). Therefore, the fact that cells with a ε-COP^{VN}•dsl1-5xWAp^{VC} BiFC pair grew well at all temperatures, and β'-COP^{VN}•dsl1-5xWAp^{VC} were viable at 30°C, shows that the BiFC formation is able suppress the negative effects of two harmful tags in the same cell.

H The main conclusion that one can draw from the results shown in the first two rows of (H) as well as panels (I) and (J) is that VC-tagged ER proteins other than the Dsl proteins cannot suppress the COPI^{VN}/*dsl1-5xWA* combination. The lack of suppressor activity is not due to weak BiFC interactions since these combinations gave BiFC signals with an intensity as high as that of the combinations used in (E) (see Fig 1G). The VN tag fused to *SEC16* slightly improved the growth of *dsl1-5xWA* cells producing α-COP^{VC}, while the equivalent ε-COP^{VC}-producing cells grew less well (compare with C). However, more samples would be necessary to prove that these minor differences are significant. The strain used in row 6 carries a BiFC combination that gave a very low fluorescence signal (Fig 1H). Both tags alone had no effect in the presence of the *dsl1-5xWA* mutation and accordingly their combination resulted in cells that grew normally at all temperatures. Row four and five of (H) summarize the growth behavior of strains that are comparable to those used in the Fig 5A and B (apart from carrying the GAL-regulated *DSL1* gene). This shows that these BiFC pairs have no effect on growth even in the presence of *dsl1-5xWA*.

I The cargo receptor Rer1p carries the VC tag at the N-terminus and is under the control of the strong RPL7B promoter (Sung & Huh, 2007). Very strong BiFC signals were observed when this VC-tagged gene was combined with genes encoding VN-tagged COPI subunits. Similarly to *SEC16*-VC and *SEC24*-VC, this VC-*RER1* did not rescue lethality of β'-COP^{VN}-producing *dsl1-5xWA* cells.

J All COPI•COPI BiFC combinations were synthetically lethal with the *dsl1-5xWA* mutation, suggesting that linking together adjacent coat complexes on vesicles is deleterious in the presence of the *dsl1-5xWA* mutation. ε-COP^{VN}•ε-COP^{VC} and δ-COP^{VN}•δ-COP^{VC} alone were temperature-sensitive. Moreover, the fact that the COPI^{VN}/*dsl1-5xWA* combination remained lethal shows again that engaging the VN tag at COPI subunits in any kind of BiFC interaction does not protect the cells from their negative effects when combined with the *dsl1-5xWA* mutation.

K The *dsl1-22* mutation, which lacks the C-terminus of domain E of Dsl1p, exhibited the same negative genetic interactions with the VN tag at COPI subunits as the *dsl1-5xWA* mutation. Moreover, this was suppressed by the VC tag at *DSL3*. Since both *dsl1* mutations behaved so similar in this assay, it is likely that the BiFC complex formation recapitulates a general function of the Dsl complex. Cells are more sensitive to higher temperatures since the *dsl1-22* mutation alone makes the cells temperature-sensitive.

L A collection of tags other than the BiFC tags was also analyzed for synthetic lethality with the *dsl1-5xWA* mutation. Note that the strongest synthetic effects were observed with GFP, which can form dimers, and RFP^{Redstar}, a tetramer-forming fluorescent protein. Together with the results shown in (J), this suggests that the mutations of *DSL1* make the cells very sensitive toward modifications of COPI subunits that link adjacent COPI heptamers and may thus delay the uncoating of vesicles.

M Combinations of the *dsl1-5xWA* defect with some temperature-sensitive COPI mutants (*sec27-1*, *ret2-1*, *ret3-1 sed28*Δ, and *sec21-1*) show that this *dsl1* defect is also synthetically lethal.

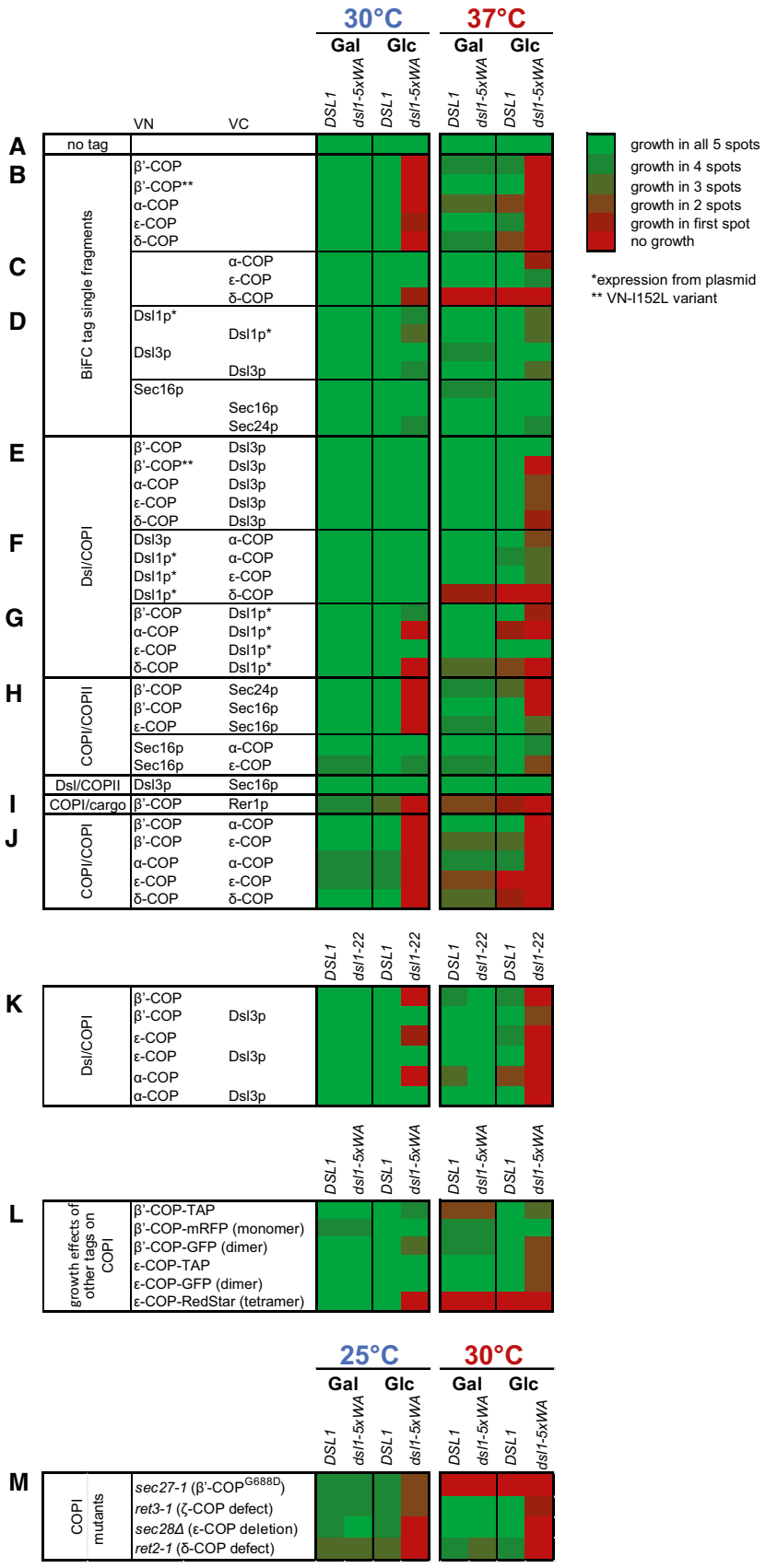
30°C
37°C
Gal
Glc
DSL1
dsl1-5xWA
VN
VC
A
no tag
B
BiFC tag single fragments
β'-COP
β'-COP**
α-COP
ε-COP
δ-COP
C
α-COP
ε-COP
δ-COP
D
Dsl1p*
Dsl1p*
Dsl3p
Dsl3p
Sec16p
Sec16p
Sec24p
E
Dsl/COPI
β'-COP Dsl3p
β'-COP** Dsl3p
α-COP Dsl3p
ε-COP Dsl3p
δ-COP Dsl3p
F
Dsl3p α-COP
Dsl1p* α-COP
Dsl1p* ε-COP
Dsl1p* δ-COP
G
β'-COP Dsl1p*
α-COP Dsl1p*
ε-COP Dsl1p*
δ-COP Dsl1p*
H
COPII/COPII
β'-COP Sec24p
β'-COP Sec16p
ε-COP Sec16p
Sec16p α-COP
Sec16p ε-COP
Dsl/COPII
Dsl3p Sec16p
I
COPI/cargo
β'-COP Rer1p
J
COPI/COPI
β'-COP α-COP
β'-COP ε-COP
α-COP α-COP
ε-COP ε-COP
δ-COP δ-COP
growth in all 5 spots
growth in 4 spots
growth in 3 spots
growth in 2 spots
growth in first spot
no growth
*expression from plasmid
** VN-I152L variant
DSL1
dsl1-22
K
Dsl/COPI
β'-COP
β'-COP Dsl3p
ε-COP
ε-COP Dsl3p
α-COP
α-COP Dsl3p
L
growth effects of other tags on COPI
β'-COP-TAP
β'-COP-mRFP (monomer)
β'-COP-GFP (dimer)
ε-COP-TAP
ε-COP-GFP (dimer)
ε-COP-RedStar (tetramer)
25°C
30°C
M
COPI mutants
sec27-1 (β'-COP G688D)
ret3-1 (ζ-COP defect)
sec28Δ (ε-COP deletion)
ret2-1 (δ-COP defect)

Figure EV2.

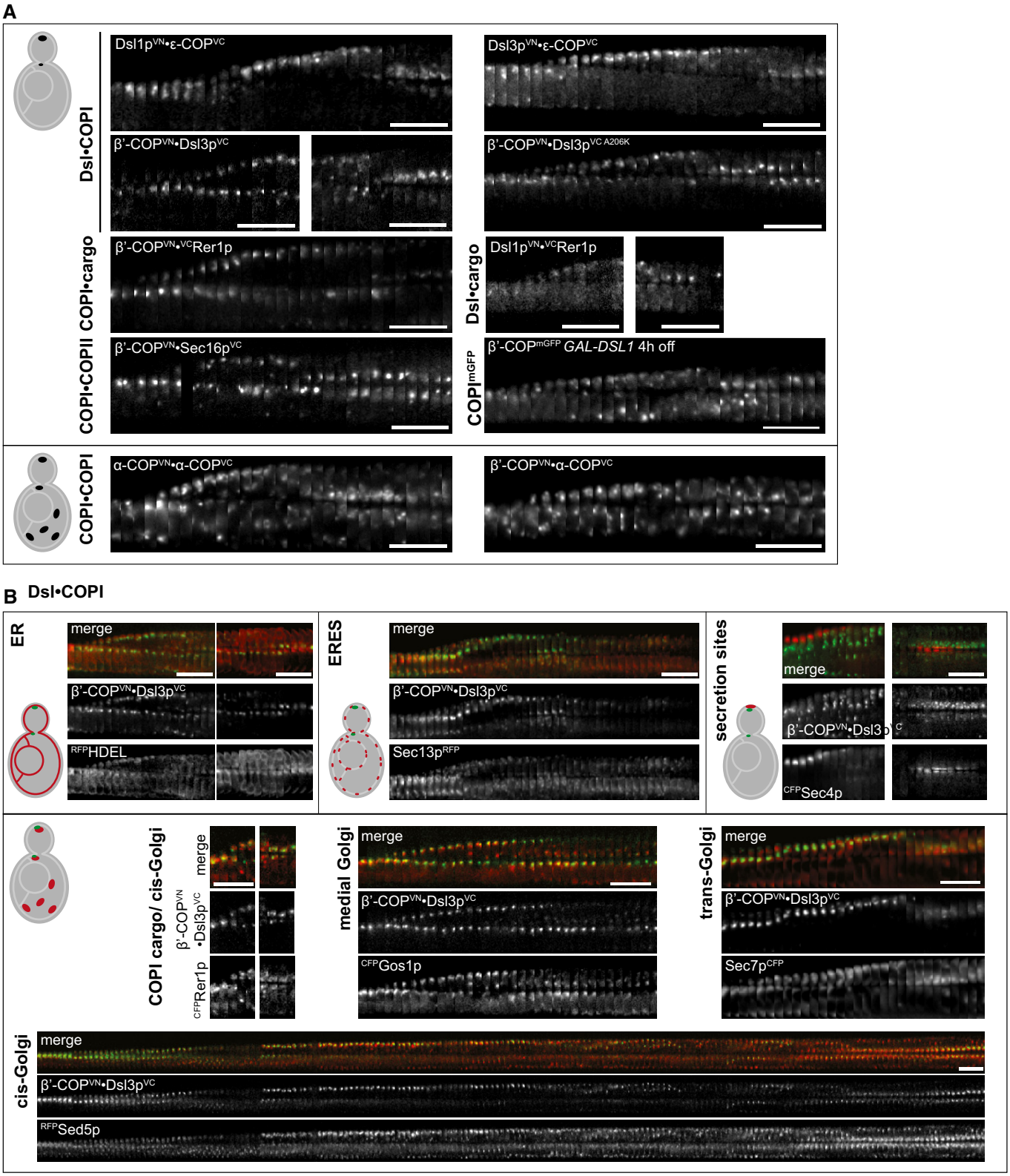

Figure EV3.

◀ **Figure EV3. Kymographs of BiFC polarization patterns and organelle association.**

Time-lapse micrographs of agarose-embedded cells were taken at RT with fresh PM Glc + ura medium supply throughout one budding cycle. Single-cell kymographs were generated by concatenating the central section of the cell (sliced along the pole axis, frames at the width of the bud neck) of one time-lapse dataset. Images were acquired at 5-min intervals, except for the datasets Dsl1p^{VN}•^{VC}Rer1p (10-min intervals) and β'-COP^{VN}•Dsl3p^{VC} + ^{RFP}Sed5p (1-min intervals). In all combinations, fluorescent foci localized to areas of membrane expansion in the bud. Frequently, another prominent fluorescent spot appeared in the mother cell on the side of the bud neck. Schematic representations of a yeast cell depict the observed fluorescence pattern in the respective strains. Scale bars, 10 μm.

A Kymographs of strains depicted in Fig 3. Cells expressing complementary BiFC-tagged proteins between subunits of the Dsl complex, the COPI complex, the COPI cargo Rer1p, the COPII complex, and the COPII adaptor Sec16p were analyzed. The combination β'-COP^{VN}•Dsl3p$^{VC\ A206K}$ contains a mutated VC tag whose alteration is equivalent to the A206K mutation in GFP, which prevents the formation of dimers (Zacharias *et al*, 2002). The COPI^{mRFP} dataset depicts β'-COP^{mRFP} fluorescence foci in Dsl1p-depleted *GAL-DSL1* cells after incubation in glucose-containing medium (YEPD) for 4 h at 30°C.

B Kymographs of strains depicted in Fig 4. In all samples, the COPI•Dsl combination β-COP^{VN}•Dsl3p^{VC} was analyzed. The cells additionally expressed organelle markers from plasmids: the ER marker ^{RFP}HDEL, the *cis*-, *medial*, and *trans*-Golgi markers ^{RFP}Sed5p, ^{CFP}Gos1p, and Sec7p^{CFP}, the COPI cargo ^{CFP}Rer1p, or the secretory vesicle marker ^{CFP}Sec4p. The ERES marker Sec13p^{mRFP} was expressed from its normal locus. BiFC signals are pseudocolored green; organelle markers are pseudocolored red. BiFC signals showed a spatial and temporal association with shown organelle markers.

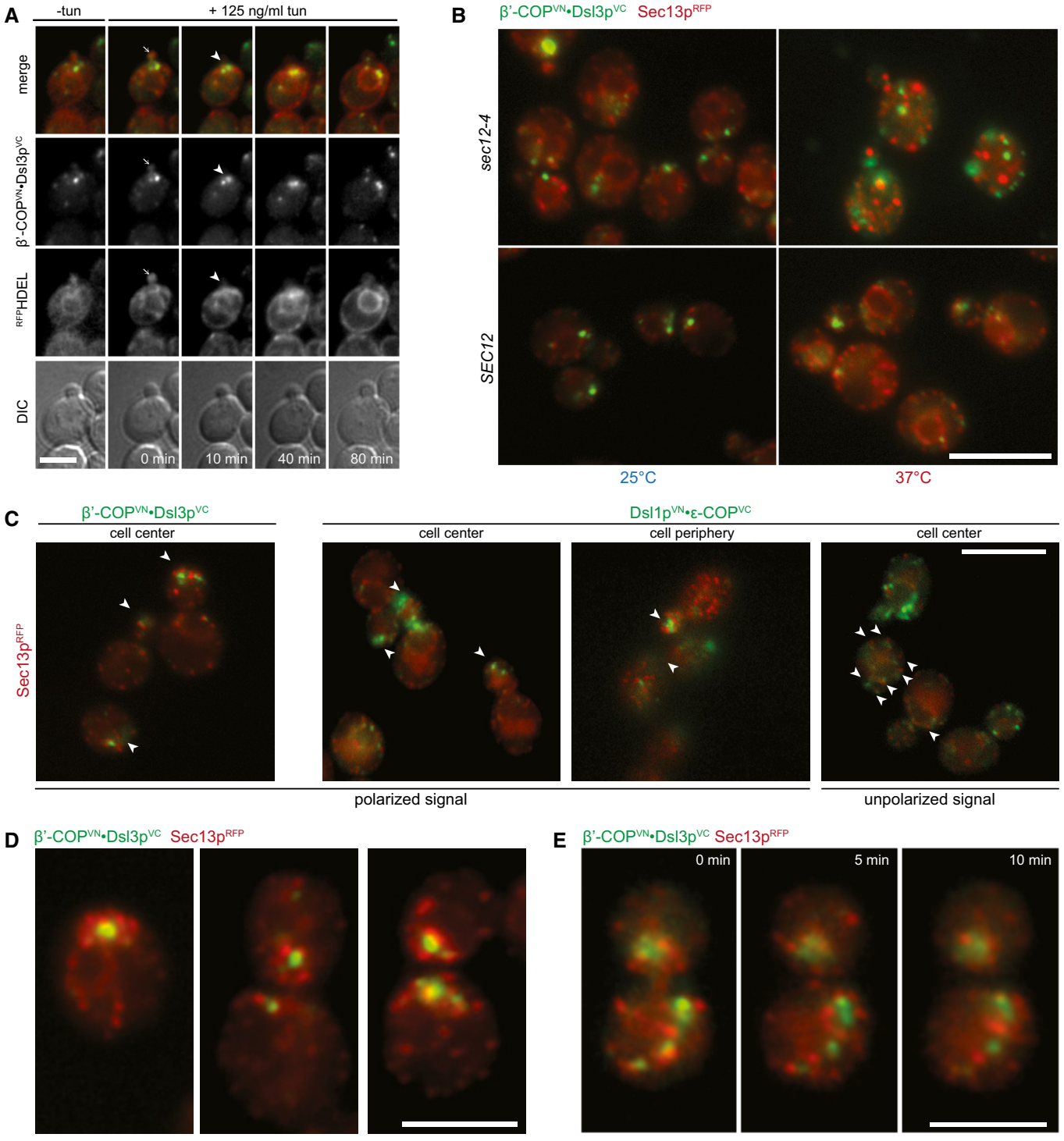

Figure EV4.

Figure EV4. ER and ERES association with ER arrival sites.

A COPI•Dsl foci association with the ER. Time-lapse fluorescence micrographs of cells carrying ER and COPI•Dsl BiFC markers. Agarose-embedded cells were grown at RT with fresh PM Glc + ura medium supply and imaged in 10-min intervals. Tunicamycin was added to the medium to a final concentration of 125 ng/ml. tubER and COPI•Dsl signals retracted simultaneously from the bud upon tunicamycin treatment. Arrows mark ER and BiFC signals in the bud, arrowheads mark loss of signals from the bud. Scale bar, 5 μm.

B ERES and ERAS coalescence. Fluorescence micrographs of cells carrying the COPI•Dsl BiFC pair β'-COP^{VN}•Dsl3p^{VC}, as well as the ERES marker Sec13p^{RFP} in a *SEC12* wild-type or *sec12-4* background. BiFC signals and ERES distribution were normal at 25°C (left panels). At 37°C (right panels), ERES aggregated in the *sec12-4* mutant, while BiFC foci lost their polarized distribution. Importantly, COPI•Dsl BiFC foci did not colocalize with coalescing ERES in the *sec12-4* mutant. Scale bar, 10 μm.

C Association of ERES and ERAS during growth and quiescence. Fluorescence micrographs of cells carrying COPI•Dsl BiFC pairs β'-COP^{VN}•Dsl3p^{VC} or ε-COP^{VN}•Dsl1p^{VC}, as well as ERES marker Sec13p^{RFP}. In fast-growing cells (panels 1-3), ERAS were polarized, and each ERAS was located in the immediate vicinity of an ERES. In non-growing cells (panel 4), ERAS were more numerous, appeared evenly distributed, and each ERAS appeared to have a corresponding ERES in immediate vicinity (arrowheads). Scale bar, 10 μm.

D, E Characteristic positioning of ERES toward ERAS in individual cells (D) or during time-lapse imaging of a single cell (E). Fluorescence micrographs of cells carrying COPI•Dsl BiFC pair β'-COP^{VN}•Dsl3p^{VC}, as well as ERES marker Sec13p^{RFP}. For (E), agarose-embedded cells were grown at RT with fresh PM Glc + ura medium. Scale bar, 5 μm.

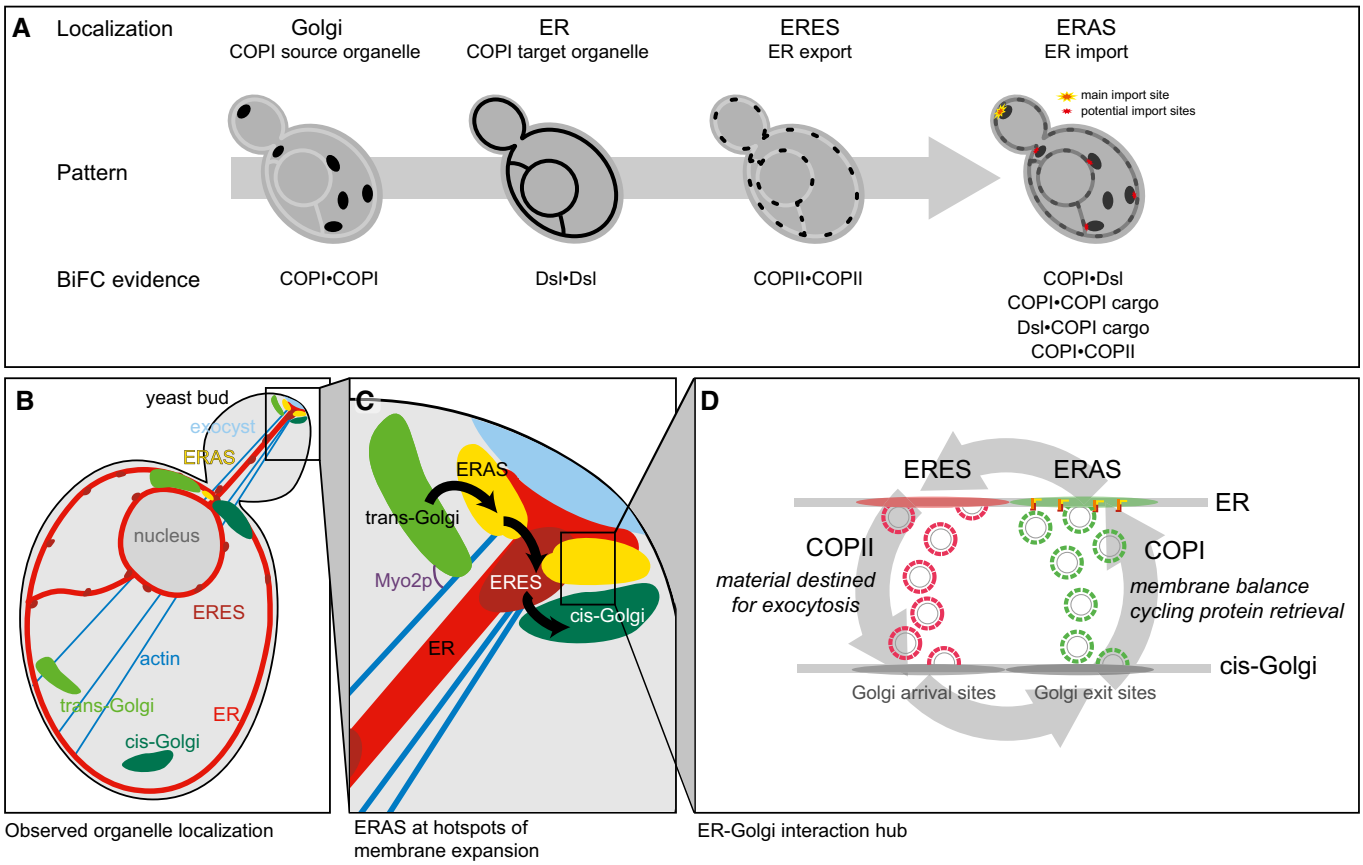

Figure EV5. Summary of findings and model for coupled material transport at the bud tip.

A Spatial arrangement of the ERAS through self-organization. BiFC results of protein complex interactions and their subcellular localization are displayed graphically. The presented data support the hypothesis that ERAS form depending on organelle localization, namely Golgi placement. ERAS localization is a logical consequence of placement of Golgi, ER, and ERES, with Golgi potentially being the critical factor.

B Schematic overview of observed subcellular localizations of organelles and interaction sites between COPI vesicles and Dsl complex (ER).

C Model of a hotspot at the bud tip. *Trans*-Golgi is transported into the bud tip via Myo2p, where it supplies the newly inherited ER with material that may be utilized for the generation of *cis*-Golgi.

D Proposed ER–Golgi interaction hub, which facilitates efficient spatially compact material exchange in anterograde and retrograde direction.